Study of Meander Line Delay in Circuit Boards

Barry J. Rubin, *Member, IEEE*, and Bhupindra Singh

***Abstract*—A moment technique is used to determine the propagation delay in meander (serpentine) delay lines located in printed circuit boards of computer systems. The full three-dimensional effects of the meander structure including signal line thickness, right-angle bends, and skin-effect are included. A set of delay lines having different pitches are considered, and results are calculated and compared to those from two-dimensional simulations, other commercial codes, analytic formulas in the literature, and experimental measurements. Based on the consistency of the results and sensitivity analyses involving numerical gridding and frequency content, the delays calculated for meander lines situated in a homogeneous medium are accurate to better than a few tenths of a percent.**

***Index Terms*—Delay line, full-wave analysis, meander, serpentine, signal integrity.**

I. Introduction

As THE CYCLE time of computer systems falls into the subnanosecond regime, the fraction of cycle time due to clock skew, associated with the synchronization of the clock signal among the logic gates, has risen. To minimize the skew, delay lines are often employed. An effective delay line should have a regular, and thus delay-predictable, shape and compact design. One popular design is the meander, or serpentine, delay line that consists of equal length segments. When the capacitive and inductive coupling between the meander segments is high and meander segment lengths are large, however, distortion in the output waveform occurs [1], [2].

To avoid severe distortion, such as steps and ripples in the signal waveform that might cause false switching of logic gates, the distance between adjacent segments (meander pitch) is kept sufficiently large to minimize coupling, but not so large as to significantly increase the area required to contain the lines. When so constrained and when the segment length is kept sufficiently short, the relatively small coupling between segments results in less delay than predicted from the total length of the lines. The effect of right-angle bends, which have been well characterized years ago by microwave engineers [3], yields a further signal speed-up that is relatively independent of meander pitch. Further, the signal line dimensions, resistivity, and frequency content of driver waveforms requires that skin-effect [4] also be considered.

High accuracy is required in calculating the propagation delay in a circuit board for computer applications. The tolerance for propagation delay in server design may be as little as 5%. Factors affecting propagation delay include tolerances in dielectric constant, the presence of other lines and vias that increase line capacitance, tolerances in board dimensions, and design issues such as meander effects. Factors that are fixed and have no random component, such as meander effects, cannot be combined in a root-mean-square fashion as can tolerances that have statistical variations. Thus, errors in predicting meander delay directly subtract from the total allowed delay tolerance. Errors of several percent, which are often quite acceptable in calculations of discontinuities, are not acceptable for meander effects in high performance computers.

Taken together, an accurate characterization of meander lines for use in computer circuit boards could not be done without a powerful analysis tool and a methodology capable of accurately extracting the required propagation parameters. It is the purpose of this paper to provide a detailed analysis of meander lines that includes meander shape, signal line thickness, right-angle bends, and frequency-dependent skin-effect. In particular, we perform a full-wave analysis of a set of meander lines that are situated between a pair of finite-sized reference planes and have various pitches. Confirmation of accuracy is provided in several ways.

We first confirm the accuracy of the solution by comparison to results generated from circuit simulations involving transmission lines whose parameters are calculated using two-dimensional (2-D) analysis. We show that simple expressions derived from the coupling between meander segments explain most of the delay variation. We then compare the numerical results to those calculated from another commercial software tool. The effect of right angle bends, or corners, is shown to explain the differences in delay predicted by our three-dimensional (3-D) moment technique and those techniques relying on 2-D analysis. We then compare results for a microstrip to experimental measurements. Sensitivity studies are also performed to quantify potential sources of error associated with numerical gridding and frequency content. Though previous investigations of the serpentine delay line have revealed individual elements of its behavior [1], [2], this is the first time a comprehensive analysis sufficiently accurate to meet the needs of computer designers has been presented.

II. Description of Meander Structures

The meander structure is shown in Fig. 1. Fig. 2 shows a top view of the entire set of meander lines. Fig. 3 gives a close-up of the 10-mil meander structure. The lines have width 3.3 mil, thickness 1.2 mil, and are composed of copper with volume resistivity of 1.84 microohm-cm. The lines are sandwiched between a pair of finite rectangular-shaped copper ground planes that extend beyond the projection of the meander lines by 10 mil in the x direction and 8 mil in the y direction. Shorting straps located 10 mil from the ends of the ground planes tie the planes

Manuscript received June 15, 2000.

B. J. Rubin is with IBM T.J. Watson Research Center, Yorktown Heights, NY 10598 USA.

B. Singh is with IBM Systems Division, Poughkeepsie, NY 12601 USA.

Publisher Item Identifier S 0018-9480(00)07411-1.

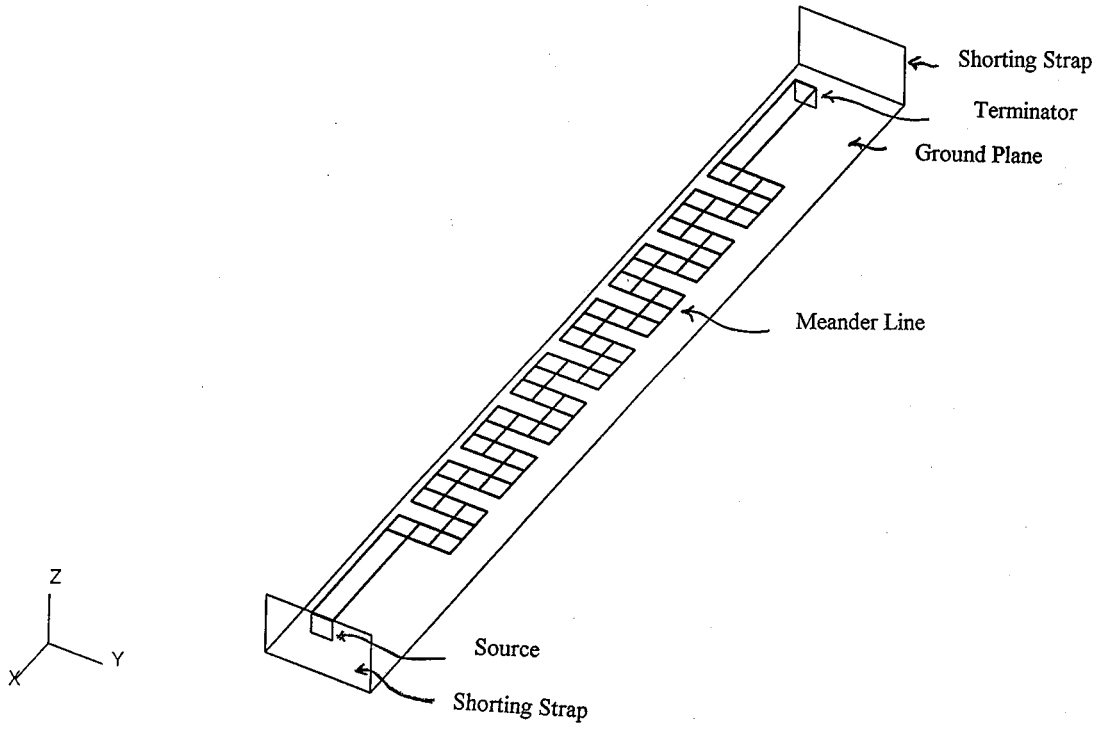

Fig. 1. View of meander delay line with top ground plane removed for clarity (not to scale).

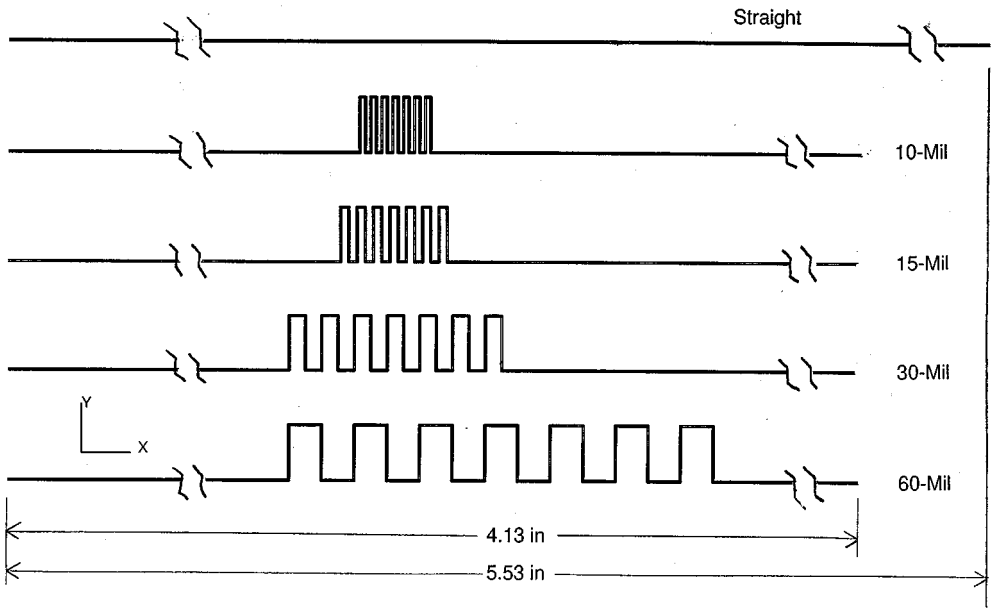

Fig. 2. Top view of set of meander lines.

together. Vertical conductive strips contain the source and terminations. The signal lines are 4.5 mil, surface-to-surface, above the lower ground plane and 10.2 mil below the top ground plane. For our analysis, the ground planes are modeled with zero thickness. The medium is homogeneous with relative dielectric constant 3.9.

All the lines were designed to have the same total length of 5.53 in, facilitating the comparison of delay between structures. They are composed of 14 meander segments, each 100 mil long, with pitches (center-center distance between the segments) of 10 mil, 15 mil, 30 mil, and 60 mil. The last is straight and serves as a reference structure since, when perfectly conducting, it is an essentially TEM structure. The structures are excited by a voltage source lying in one conductive segment and terminated in another conductive segment (Fig. 1). Source and termination resistances are 50 Ω, which nearly match the characteristic impedance of the straight line structure (about 58 Ω).

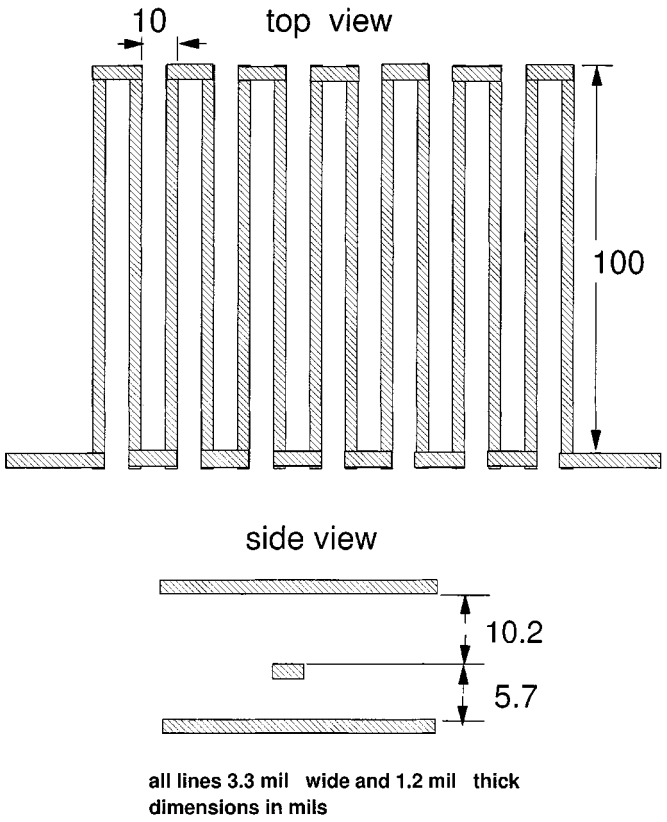

Fig. 3. Top and side view of 10-mil meander line structure.

The source is a 2-V square wave having 50% duty cycle and rise and fall times of 0.2 ns. To analyze the structure we employ a moment method solution, where results are calculated in the frequency domain and converted to the time domain through appropriate use of Fourier series. Because the structure is nearly terminated, the reflections decay within a few round-trip crossings of the structure; a 5-ns period is adequate. Our input waveform has quarter-wave symmetry so that only odd harmonics are needed, starting from the first harmonic at 0.2 GHz, and we assume a cut-off frequency of 4 GHz.

III. Analysis

The EMSIM code, a full-wave analysis code originally intended for electromagnetic interference (EMI) calculations and previously available through the Pacific Numerix Corporation, was used for the analysis. As described in [5] and [6], EMSIM is a moment method technique that employs rooftop basis functions and line-integral testing. Though the original reference describes a solution based on a uniform grid, refinements in the code have extended this to nonuniform grids. Further improvements include an automatic gridding facility that modifies the subsection sizes to account for proximity and frequency effects. A delta-gap voltage source, which is an impulse of electric field whose line integral along a specific direction is 1 V, provides the excitation at each harmonic. Voltages are determined by the current through the termination resistances. Skin- effect is also included.

Perhaps the most accurate way to account for skin-effect is to subdivide the conductor volume into subsections, with appropriate sections smaller than the skin depth. However, at higher frequencies the skin depth is only a small fraction of the signal line thickness. Employing a uniform grid would yield over 100 000 unknowns, far greater than can be accommodated by moment method codes on a typical workstation. A nonuniform gridding of the conductor volume, though requiring fewer unknowns, would still be impractical. Instead, we employ a surface-based approximation.

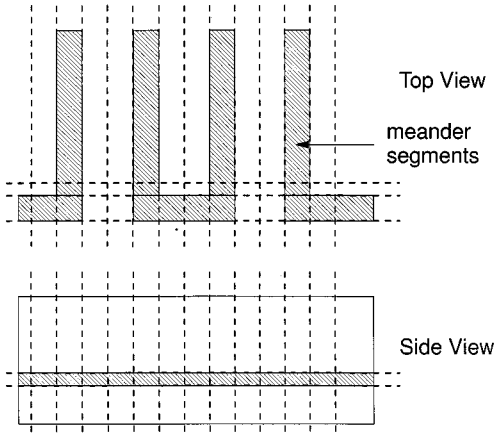

Fig. 4. Grid lines (shown dashed) associated with individual grid for a section of the 10-mil meander structure.

An appropriate surface impedance [7] is applied to all conductors, including the ground planes. The surface impedance is frequency-dependent and given by $(1+j)R_s$, where R_s is the material resistivity divided by the skin depth. For copper, the skin depth at the lowest frequency (0.2 GHz) is 0.19 mil, or about one-sixth of the signal line thickness, while at our 4-GHz cutoff frequency, the skin depth is 0.042 mil, or one twenty-eighth the thickness. The approximation is adequate at lower frequencies, as later shown in Section IV-E, but is especially good at the higher frequencies. From Fourier analysis, the higher frequencies are critical in defining the sharp edges of the waveforms that are responsible for determining delay.

The numerical grid for the lossless 10-mil meander structure is determined first. We apply the criteria that the maximum size of any subsection is less than 0.1 wavelength in the dielectric. A projection gridding scheme is employed, and this means, for example, that any grid lines associated with the meander segments project and appear on the ground planes as well. Additional grid lines are added at regions determined by the proximity of conductors. The gridding in the x–y plane for a section of the structure is shown in Fig. 4 through the dashed lines. Similar grids are used for the meander lines of other pitches. About 3660 unknowns are required for the analysis.

To get an idea of the numerical error in delay associated with the subsection size, we also analyzed the 10-mil, 15-mil, and 30-mil structures using a grid formed by the superposition of the individual grids, projecting the grids for these three structures onto the x–y plane and combining them. Because the same grid is used for each structure, differences in delay are independent of the gridding.

Fig. 5 shows the input and output voltage waveforms for the 10-mil meander structure. The voltage waveform starts rising at

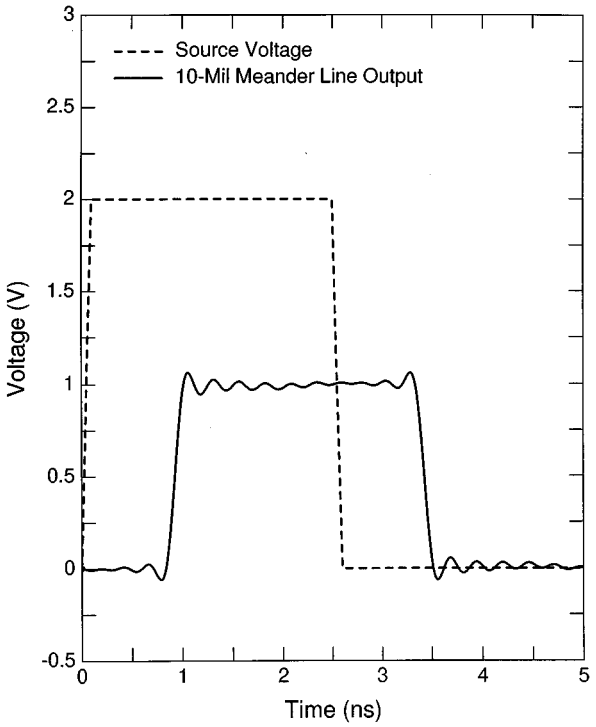

Fig. 5. Input and output voltage waveforms for lossless 10-mil meander line.

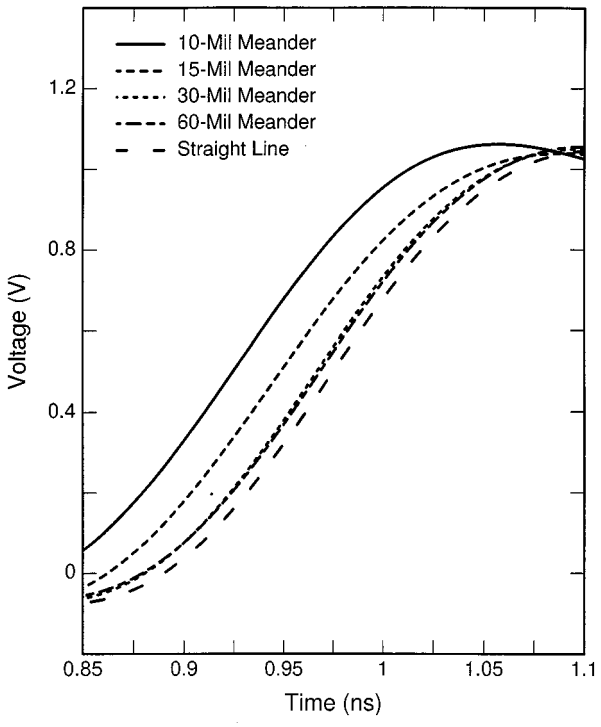

Fig. 6. Output voltages for lossless meander set calculated using individual grid.

$t = 0$ ns and the output waveform, delayed the propagation time through the structure, starts rising about 1 ns later. The waveforms are periodic, and only the voltages in one period are shown. The delay is determined from the crossing of the input voltage source through 0.5 V, which occurs at exactly 0.1 ns, and the crossing of the output waveform through 0.5 V. We chose to use this criteria for delay because it corresponds closely with the TEM delay for the total line length.

The ripples are associated with the Gibbs phenomenon, which refers to the difficulty of a Fourier series to represent a waveform near discontinuous regions; in our case it occurs during the time period around the rise and fall transitions. The ripples are reduced in amplitude as the number of included harmonics is increased. Fig. 6 shows the output waveforms, expanded in the vicinity of $t = 1$ ns, for the set of lossless meander lines.

IV. Numerical Results

A. Moment Method Solution of Meander Set

The delays are extracted from the output waveforms and presented in Table I, where the delay for the straight line (base delay) is subtracted from each entry. Delay is minimal for the smallest pitch and increases with pitch; the negative values indicate a speed-up with respect to the straight line. The delay through the straight line (926 ps) is very close to that of a TEM structure of the same length (925.3 ps). In the following discussions, we refer to the difference between the delay of a meander line and the delay of a corresponding, equal length, straight line as the relative delay. This terminology allows us to more easily concentrate on the primary parameter of interest, namely the speed-up observed in meander lines.

TABLE I
Relative Delay for Meander Structures

Structure	Lossless, Indiv. Grid Relative Delay(ps)	Lossless, Composite Grid Relative Delay(ps)	Lossy, Composite Grid Relative Delay(ps)
Base Delay	(926)	(926)	(941)
Straight	0	0	0
60-Mil Meander	---	-7.5	-----
30-Mil Meander	-9.5	-8.5	-9.5
15-Mil Meander	-25.5	-25.5	-25.0
10-Mil Meander	-51.5	-51.5	-51.5

The meander line with tightest pitch (10 mil) displays a speed-up of 51.5 ps. Considering that meander segments represent only 1.4 in out of the total length of 5.53 in, the speed-up in the meander region is about 22%. For the greatest pitch (60 mil), the delay reduction is 7.5 ps; the coupling between the parallel sections of the meander line is negligible at this pitch, which means that the delay reduction is caused by the right-angle bends. The calculated delays are essentially the same for the individual and composite grids; this gives us confidence that the results are insensitive to gridding and thus highly accurate.

From Table I, the delays for the lossy meander structures are about 2% greater than for the corresponding lossless structures, with relative delays that are virtually the same. This 2% increase in delay was confirmed through a skin-effect analysis of a straight line obtained by 2-D quasi-static modeling and the transmission line analysis facility of the ASTAP program [8].

In a second set of runs, a cutoff of 8 GHz was employed for the lossy structure, which not only doubled the number of harmonics but halved the maximum subsection size, in accordance with the 10 subsections per wavelength gridding criteria. For the

straight line, 10-mil, and 30-mil structures, the delay increased, respectively, by 5.0 ps, 6.0 ps, and 5.5 ps. The variation in relative delays was thus 1 ps, or about 0.1% of the total delay. Since bus frequencies typically appearing on a circuit board correspond to only a fraction of the clock speed, we see no need to find the sensitivities at frequencies higher than 8 GHz.

B. Solution Using 2-D Capacitance Calculation and Circuit Simulation

A 2-D electromagnetic analysis is performed to calculate, for the purposes of circuit simulation, the parameters of the coupled line structure formed by just the 14 meander segments. Because these segments form a TEM structure, the inductive coupling equals the capacitive coupling and both may be obtained from a 2-D capacitance calculation. A simplified schematic (Fig. 7) shows the coupled transmission line, voltage source, and source and termination resistances, $R_{\rm in}$ and $R_{\rm out}$, which are each 50 Ω. The circuit is then analyzed using the ASTAP circuit program. The results are presented in Table II, along with the coupling calculated by the 2-D analysis and a hand-calculation of the delay based upon the coupling that we now describe.

When the delay across a meander segment is small compared to the risetime of the input waveform, the voltages on adjacent segments are nearly the same. The capacitance of each meander segment is reduced by the coupling capacitance to the adjacent segments. Similarly, the currents in adjacent segments are in opposite directions, yielding an inductance for each segment that is reduced by the mutual inductance to each adjacent segment. If we calculate delay as the square root of the product of the capacitance and inductance, and recognize that the capacitive and inductive couplings are the same, as discussed above, we can calculate the delay in terms of the capacitive coupling. For example, if the ratio of coupling capacitance to self-capacitance is 0.10, then the capacitance of a meander segment surrounded by two other meander segments is reduced by about a factor of 0.2. This gives rise to about a 20% speed-up in the propagation across the meander structure. The hand calculations (last column of Table II) account for coupling between only adjacent meander segments and that the first and last segments are coupled to only one other segment, not two.

From Table II, we observe that the delay calculated by the circuit approach varies with signal risetime due to laddering [1], [2], though not excessively. The circuit-calculated results agree quite well with the hand calculation, though the hand-calculation does not account for associated waveform laddering. The speed-ups in Table II are smaller than those in Table I, especially for the larger pitches. These differences are due to the right-angle bend (corner) effect, and, in fact, can be seen directly from the Table I entries for 60-mil pitch. A fairly accurate prediction of the meander effect may thus be obtained by finding the capacitive coupling between two adjacent meander segments, finding the right-angle-bend effect through formulas such as those in [3] and calculating the speed-up through the summation of these two effects.

The Speed97 analysis program [9] from Sigrity was then used to calculate the propagation delay for the same set of meander lines. Though it handles many of the physical effects associated with meander lines and provides the solution far faster, it does not include 3-D corner effects of bends automatically; if equivalent circuit models of 3-D corners are extracted beforehand, however, they can be inserted at the location of the bends. Speed97 handles coupling between adjacent lines but is limited in handling losses of the lines due to proximity effects [10]. The delays calculated without equivalent circuits inserted for corners are shown in Table III and agree well with our results. The omission of corner effects is clearly indicated by the small relative delay of -1.0 ps for the lossless 30-mil meander line. The corresponding difference of 8.5 ps between Speed97 and EMSIM is again the corner effect. The difference is about the same, namely 8.0 ps for the 15-mil pitch, but only 0.6 ps for the 10-mil pitch. Though agreement for each pitch is better than 1% of the total delay, the variations from 8.5 ps to 0.6 ps indicate that the differences are due to more than corner effects. For the lossy case, the results also agree closely, although we do not understand why the difference in relative delay between lossless and lossy cases for Speed97 increases from 0.1–3.8 ps as pitch is reduced.

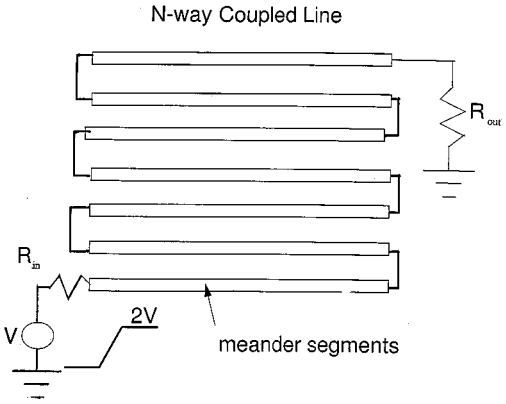

Fig. 7. Schematic of circuit used for 2-D simulation of meander lines.

TABLE II
RELATIVE DELAY FOR 14 LOSSLESS MEANDER SEGMENTS, BASED ON CIRCUIT ANALYSIS

30 Mil Meander	-0.2	-0.2	-0.1	0.0%	0
15 Mil Meander	-17.4	-18.1	-12.9	4.2%	-18
10 Mil Meander	-46.7	-41.9	-39.1	11.5%	-50

TABLE III
RELATIVE DELAY COMPARISON BETWEEN SPEED97 AND EMSIM

Structure	Lossless Speed97 Relative Delay(ps)	Lossy Speed97 Relative Delay(ps)	Lossless EMSIM Relative Delay(ps)	Lossy EMSIM Relative Delay(ps)
Base Delay	(927)	(932)	(926)	(941)
Straight	0	0	0	0
30 Mil Meander	-1.0	-0.9	-9.5	-9.5
15 Mil Meander	-17.5	-16.9	-25.5	-25.0
10 Mil Meander	-50.9	-47.1	-51.5	-51.5

C. Focus on Corner Effects

The corner effect, as seen from the 30-mil and 60-mil entries in Table I, is about 8 ps. To confirm this effect, we employ formulas provided through [3, Fig. 8, Appendix A-4]. These formulas give the excess capacitance and inductance for a zero-thick line situated halfway between two infinite ground planes. We then use EMSIM to calculate the delay for a 60-mil-pitch

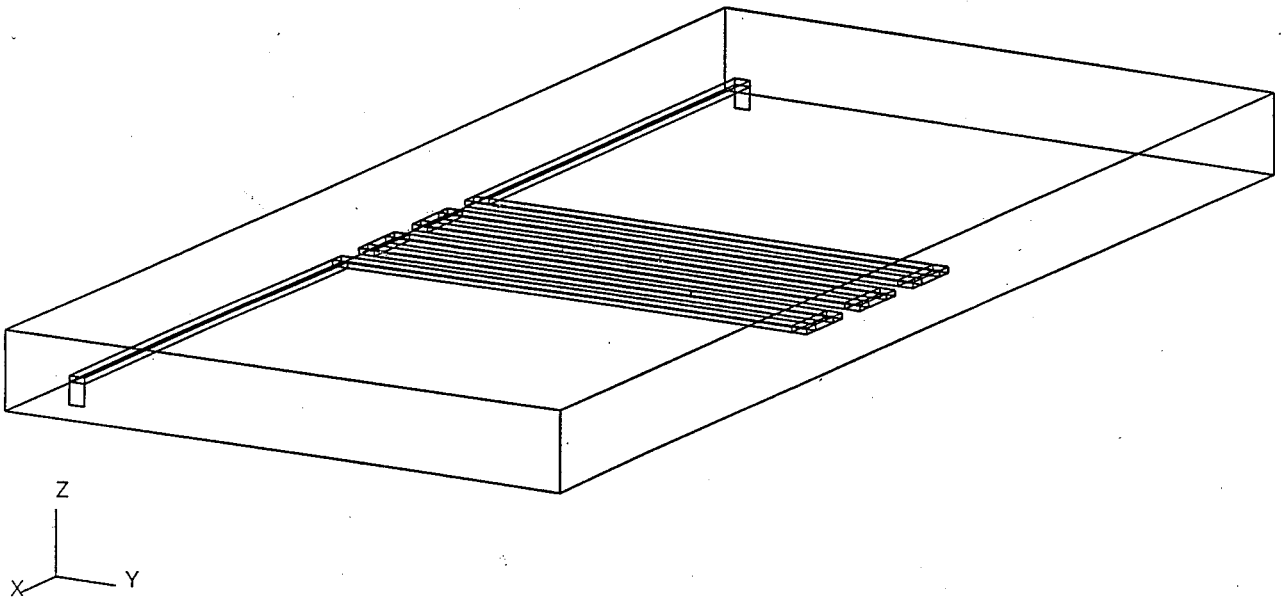

Fig. 8. Reduced 10-mil meander structure used for grid sensitivity analysis.

meander line that is 0.4-mil thick and situated halfway between two zero-thick ground planes separated by 9.4 mil. A small, as opposed to zero, trace thickness is employed because the presence of sidewall currents on the trace allows for greater accuracy. We obtain a speed-up of 6.1 ps.

The variational formulas [3] show that, over our frequency range, the excess capacitance is positive but negligible and that the excess inductance is significant and negative. The first formula from Appendix A-4, after dropping the small, frequency-dependent term, becomes

$$X_a/Z_o = 2(0.878)D/\lambda \tag{1}$$

where X_a is an inductive reactance, Z_o is the characteristic impedance of the trace, λ is the wavelength, and D is the effective width for the trace. The effective width accounts for striplines that are not ideal parallel plates. From the reference formula 1b, with plate separation $b = 9$ mil and trace width $w = 3.3$ mil, D is 7.27 mil.

Using (1), we then make the following substitutions:

$$X_a = 2\pi f L_a$$
$$\lambda = \nu/f$$
$$Z_o = \nu L$$

where L_a is an inductance, f is frequency, ν is the velocity of light in the medium, and L is the per unit length inductance of the trace. From the figures and equivalent circuit in the reference, the length of the corner is D and the total inductance of the corner is $2L_a$. Thus, the corner inductance after substitutions into (1) is

$$2L_a = 2(0.878)LD/\pi = 0.559\,DL. \tag{2}$$

The TEM delay for a length of 7.27 mil is 1.216 ps. The delay for a corner, based on (2) and after taking the square root of the 0.559 factor, is 0.912 ps, giving a speed-up per corner of 0.30 ps or 8.4 ps for 28 corners. Had we taken the excess inductance per corner, which from (2) is -0.441 DL, and added 28 of these contributions to the total meander line inductance, the speed-up based on this distributed calculation would have been 7.6 ps.

Thus we estimate the speed-up predicted from the reference as between 7.6–8.4 ps, which reasonably confirms our 6.1 ps speed-up calculated through the moment method. Remember that this modified structure involves a symmetric stripline, and thus the vertical dimensions differ from those in Fig. 3. It is also important to realize that planned or unplanned processing variations that cause the corner to be other than perfectly rectangular will impact delay. A chamfered corner [11] can be used to increase delay and thus compensate for the speed-up.

D. Sensitivity Studies on Gridding

Sensitivity studies were performed on a reduced-length 10-mil meander structure (Fig. 8) to quantify the error due to gridding. The reduced structure permits subsequent gridding refinements without leading to an excessive number of unknowns. The structure consists of six meander segments and straight line segments that are only 98.35 mil long. The grid was initially similar to that in Fig. 4 and then halved along the x and y directions. The base delay is 326 ps. The variation in delay as gridding was refined less than 0.1 ps. The above gridding studies involve changes to the gridding outside the signal line region. Only one subsection is employed along the width and one along the thickness, giving rise to four subsections around the perimeter of the signal line.

To assess the effects of gridding within the signal line region on skin-effect, we reconsider the straight line structure (Fig. 2). We expect the variation in delay due to skin-effect to be similar for straight and meander structures, with perhaps some minor difference due to the corners. Starting from an edge of the signal line and moving inward along the signal line's top or bottom

surface to its center, extra grid lines were placed at 1 , 3 , 7, and 15 μm from the edge; starting from an edge and moving along the signal line's sides, extra grid lines were placed at 1 , 3 , and 7 μm from the edge. This fine gridding provides 32 sections along the perimeter, and should be satisfactory to account for any increased resistive losses associated with currents near the edges.

The variation in delay between the coarse and finely gridded structures is less than 1 ps. Thus, the original individual grid is perfectly adequate for skin-effect modeling. Care must be taken in extrapolating the delays calculated from reduced-length structures, however, because the effect of line resistance is not linear with respect to length and may be far more pronounced on longer structures.

E. Sensitivity Study for Skin-Effect

A 2-D quasi-static analysis [12] was performed on the cross section of the straight line to obtain the per unit length inductance L and resistance R. By comparing these results to those calculated from our moment technique, we can confirm the validity of the surface approach at the equivalent circuit level. We first confirmed through convergence studies that the quasi-static results are accurate to within 1%.

The EMSIM program was employed in conjunction with a port extraction facility [13] to obtain L and R. In the extraction, a section of the straight signal line is excited by impulse voltage sources at each end of the line and the current on the signal line and voltages between the signal line and reference planes are calculated at two "port" planes. The port planes are fictitious and similar to those employed in microwave analyses to extract discontinuity effects from waveguides. They are chosen to be situated sufficiently far from the sources and sufficiently far from any discontinuites that the fields around the port planes are nearly uniform. This permits voltages to be calculated through line integration of the electric field.

The entire structure is 1 cm in length and port planes are located at 0.49 cm and 0.51 cm. As described in [13], the Y-matrix is extracted and the RLCG values are obtained. Because the same full-wave approach and skin- effect modeling are employed in the meander analysis and in the port extraction, insight into the accuracy of skin-effect modeling can be gained by investigating the port-extracted values. Table IV gives the R and L values. The port extraction procedure is performed for a coarse grid, consistent with four sections around the perimeter of the signal line, and for a fine grid, employing 32 sections around the perimeter.

As seen from the table, the port-extracted values for frequencies greater than 0.1 GHz, even for the coarse grid, are well within 20% of the values obtained by the quasi-static approach. Though the port-extracted values at lower frequencies are clearly incorrect, this is inconsequential for the meander analysis because frequencies below 0.2 GHz (first harmonic) do not appear in the delay simulations. Because the difference between the results for coarse and fine gridding are only a few percent, the coarser grid is perfectly adequate. We now compare results for a microstrip meander line with those previously measured by Wu and Chao [1].

TABLE IV
PER UNIT LENGTH RESISTANCE AND INDUCTANCE FROM QUASI-STATIC AND PORT EXTRACTION APPROACHES

Frequency	Quasi-Static		Port Extraction (Coarse)		Port Extraction(Fine)	
(GHz)	R(Ω/cm)	L(nH/cm)	R(Ω /cm)	L(nH/cm)	R(Ω /cm)	L(nH/cm)
0.001	0.0776	4.7074	0.0142	6.3405	0.0142	6.2445
0.01	0.0856	4.4079	0.0472	4.7249	0.0473	4.6264
0.1	0.1927	4.0996	0.1584	4.1840	0.1595	4.0830
1.0	0.5842	3.9060	0.5229	4.0037	0.5360	3.8996
10.0	1.8301	3.8436	2.0268	3.9637	2.1272	3.8570

F. Microstrip Meander Line and Experimental Measurements

The meander structure in [1] has traces with 5.5-mil by 1.13-mil cross section, an 11.5-mil meander pitch, and nine meander segments each 3-cm long. The total length of this meander structure, based on distance along the centerline of the traces, is 27.25 cm. The lines are located 5.735 mil above a 1.13-mil thick ground plane, with a dielectric extending 13 mil above the ground plane. The conductors have a conductivity of 6.5 Ω/m. The relative dielectric constant is 4.5 and the loss tangent of the dielectric material is not specified; we assume it to be zero. The risetime of the input waveform used in the measurements was 0.35 ns.

For our analysis, we employed a 20-ns period and a cutoff of 4 GHz. Because our approach requires six unknowns to model the polarization current in each dielectric cell generated during gridding [6], we had to use a relatively coarse grid to avoid an excessive number of unknowns. This leads to an artificial increase of about 12.5% in self-capacitance of the meander segments, which in turn leads to larger than expected delays. This limitation was circumvented by using a modified value of 4.02 for the relative dielectric constant, which through 2-D capacitance analysis was found to give the correct value of self-capacitance. This is not an issue for the meander set, which involves homogeneous dielectrics, as we have shown accuracy to within about 0.1%.

The comparison is shown in Fig. 9. The rise transition and amplitudes of the peaks and valleys agree nicely with those from Wu, though the steps in waveform due to the laddering are less pronounced. (Our meander set showed no such steps because their segment lengths normalized by dielectric constant and rise time were only one-seventh as long.) The distances between the relative peaks and valleys are greater in our results, even after correction of the dielectric constant. If this effect is still related to the coarse gridding for the dielectric, it would appear in all meander structures and could be minimized by normalizing the relative delay by the absolute delay.

We would also like to point out that as valuable as measured data is to confirm physical effects, it would not be sufficiently accurate to determine the fine differences in delay between meander lines of different pitch. Variations in dielectric constant, trace cross sections and dielectric thicknesses can be fairly high, and this has become clear from efforts to design printed circuit boards with well-controlled impedances [14]. Even a 5% variation in dielectric constant would lead to an uncertainly of a few percent in measured delay, and this exceeds the less than 1% difference between say a 15- and

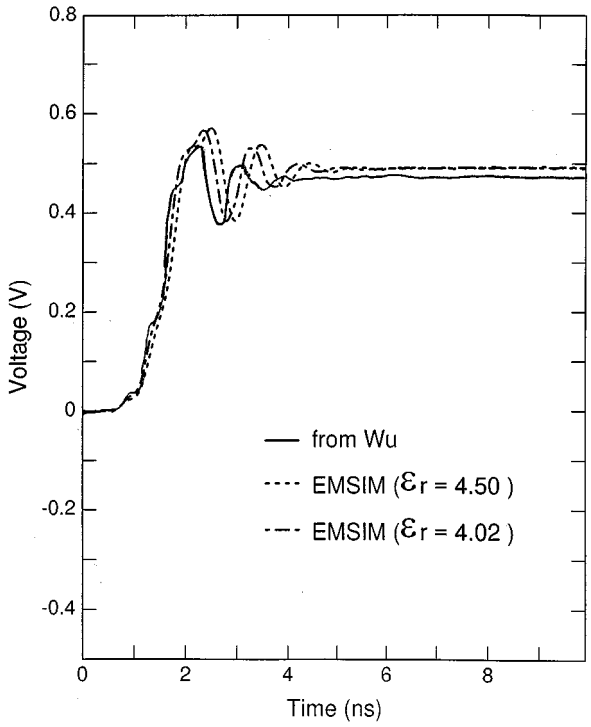

Fig. 9. Comparison of calculated and measured waveforms for microstrip meander structure.

30-mil meander line. Such parameter variations may also account for at least some of the difference between calculated and measured results in Fig. 9.

V. Discussion and Conclusions

A comprehensive full-wave analysis of a set of meander delay lines was performed. Both individual grids and a composite gridding strategy were employed, with variations in delay of less than 0.1% observed. A second study performed on a reduced 10-mil-meander structure also yielded errors in absolute delay of less than 0.1%. Such small differences in delay are expected and consistent with generic convergence studies. Capacitance and inductance typically move in opposite directions as gridding is made finer, so that their product and thus delay tends to remain constant.

Studies were also performed to check the validity of the surface impedance approach in modeling skin-effect. Gridding studies showed that a coarse grid on the signal line surface is perfectly adequate and that the resistance and inductance for lossy structures obtained from the full-wave approach agrees well with those based on quasi-static analysis. The variation of relative delay with cut-off frequency was found to be small.

Confirmation on the qualitative speed-up associated with the meander structure was obtained by use of a 2-D capacitance analysis and subsequent circuit analysis. The speed-up due to the corner effect was confirmed directly through auxiliary calculations of a thin meander structure and predictions in delay based on variational formulas. Taken together, these studies strongly indicate that the relative delays calculated for meander lines situated in homogeneous regions are highly accurate.

A comparison was done with experimental measurements. Agreement was reasonable, especially after an adjustment was made to compensate for insufficient gridding of the dielectric region. The differences associated with the steps due to laddering are not an issue in precision delay lines, since segments long enough to cause steps would not be used in the first place. Though accuracy in absolute delay for microstrips is clearly less than for homogeneous structures, a normalization of the relative by the absolute delay will improve the accuracy.

Because typical process variations could lead to a several percent variation in two samples of the same structure, extreme effort would be needed to accurately determine through measurement the difference in delay between meander lines of different pitch. Use of glass substrates and averaging over many samples, at a minimum, would be needed. Thus, analytical techniques may be preferable for the determination of relative delay for meander lines of different pitches. Based on the studies contained in this paper, the full-wave approach is highly accurate and well-suited to the task of defining meander lines to trim clock skew.

References

[1] R. Wu and F. Chao, "Laddering wave in serpentine delay line," *IEEE Trans. Compon. Packag., Manufact. Technol.*, vol. 18, pp. 644–650, Nov. 1995.

[2] R. Wu and F. Chao, "Flat spiral delay line design with minimum crosstalk penalty," *IEEE Trans. Compon. Packag., Manufact. Technol.*, vol. 19, pp. 397–402, May 1996.

[3] A. Oliner, "Equivalent circuits for discontinuities in balanced strip transmission line," *IRE Trans. Microwave Theory Tech.*, vol. MTT-3, pp. 134–143, 1955.

[4] A. Deutsch *et al.*, "High-speed signal propagation on lossy transmission lines," *IBM J. Res. Develop.*, vol. 34, pp. 601–615, 1990.

[5] B. J. Rubin and S. Daijavad, "Radiation and scattering from structures involving finite-size dielectric regions," *IEEE Trans. Antennas Propagat.*, vol. 38, pp. 1863–1873, Nov. 1990.

[6] B. J. Rubin, "Divergence-free basis for representing polarization current in finite-size dielectric regions," *IEEE Trans. Antennas. Propagat.*, vol. 41, pp. 269–277, Mar. 1993.

[7] A. Otteni, "Plane wave reflection from a rectangular-mesh ground screen," *IEEE Trans. Antennas Propagat.*, vol. AP-21, pp. 843–851, 1973.

[8] "Advanced statistical analysis program (ASTAP)," in *Program Reference Manual*. White Plains, NY: Data Processing Division, IBM Corp., 1973.

[9] Y. Chen, Z. Chen, Z. Wu, D. Xue, and J. Fang, "A new approach to signal integrity analysis of high speed packaging," in *4th Topical Meeting Elect. Performance Electron. Packag.*, Oct. 2–4, 1995, pp. 235–238.

[10] Correspondence with Jiayuan Fang, Mar. 24, 2000.

[11] Bahl and Bhartia, *Microwave Solid-State Circuit Design*. New York, NY: Wiley, 1988, ch. 2.

[12] W. T. Weeks, L. L. Wu, M. F. McCallister, and A. Singh, "Resistive and inductive skin effect in rectangular conductors," *IBM J. Res. Develop.*, vol. 23, pp. 652–660, 1979.

[13] B. J. Rubin and S. Daijavad, "Calculation of multi-port parameters of electronic packages using a general purpose electromagnetics code," in *2nd Topical Meeting Elect. Performance Electron. Packag.*, Oct. 20–22, 1993, pp. 37–39.

[14] R. Evans, J. Diepenbrock, and R. Sharrar, "Implementation considerations for RAMBUS™-based systems," in *8th Topical Meeting Elect. Performance Electron. Packag.*, Oct. 25–27, 1999, pp. 25–27.

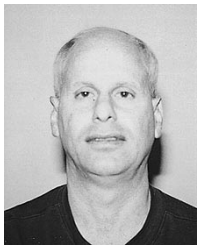

Barry J. Rubin (S'72–M'74–M'82) received the B.E.E.E. degree from the City College of New York in 1974. In 1978, he received the M. S. degree from Syracuse University, Syracuse, NY, and, in 1982, the Ph.D. degree from the Polytechnic Institute of New York, both in electrical engineering.

He first joined IBM in 1974 at its East Fishkill Facility, Hopewell Junction, NY. In 1986 he transferred to IBM's T. J. Watson Research Center, where he is currently involved in the electromagnetic modeling of computer packages. He has worked on power transistor design, CCD technology, circuit design, and since 1976, on all aspects of electrical package analysis. He continues to work on novel analytic techniques for the accurate and robust calculation of electrical packaging parameters and is also known for his contributions as the primary developer of the commercially available EMSIM analysis tool. He has been awarded a number of patents on circuit and package-related devices.

Bhupindra Singh received the B.S.E.E. degree from Punjab University, Chandigarh, India in 1966 and the M.S.E.E. degree from Syracuse University, Syracuse, NY in 1978.

He is an Advisory Engineer at IBM S/390 Division, Poughkeepsie, NY. He is currently working in advanced VLSI and packaging applications. He is involved in design, modeling, and noise simulations of high-performance multi-chip and single-chip packages.